Non-Repeatability, Scale- and Model Effects in Laboratory Measurement of Impact Loads Induced by an Overtopped Bore on a Dike Mounted Wall

Streicher, Maximilian; Kortenhaus, Andreas; Altomare, Corrado; Hughes, Steven; Marinov, Krasimir; Hofland, Bas; Chen, Xuexue; Suzuki, Tomohiro; Cappietti, Lorenzo

DOI
10.1115/OMAE2019-96703

Publication date
2019

Document Version
Accepted author manuscript

Published in
ASME 2019 38th International Conference on Ocean, Offshore and Arctic Engineering

Proceedings of the ASME 2019 38th International Conference on Ocean, Offshore and Arctic Engineering
OMAE2019
June 9-14, 2019, Glasgow, Scotland

OMAE2019-96703

NON-REPEATABILITY, SCALE- AND MODEL EFFECTS IN LABORATORY MEASUREMENT OF IMPACT LOADS INDUCED BY AN OVERTOPPED BORE ON A DIKE MOUNTED WALL

Maximilian Streicher[1], Andreas Kortenhaus
Dept. of Civil Engineering, Ghent University, Technologiepark 904, B-9052 Zwijnaarde (Ghent), Belgium

Corrado Altomare[2]
Maritime Engineering Laboratory, Universitat Politecnica de Catalunya, carreer Jordi Girona 1-3, 08034 Barcelona, Spain

Steven Hughes
Engineering Research Center, Department of Civil and Environmental Engineering, 1320 Campus Delivery, Colorado State University, CO 80523-1320 Fort Collins, USA

Krasimir Marinov
Fac. of Hydraulic Eng., Univ. of Architecture, Civil Eng. and Geodesy, Hristo Smirnenski 1 Blvd, 1046 Sofia, Bulgaria

Bas Hofland
Faculty of Civil Engineering and Geosciences, Delft Uni. of Technology, Stevinweg 1, 2628 CN Delft, The Netherlands

Xuexue Chen
HaskoningDHV Nederland B.V, George Hintzenweg 85, 3068AX Rotterdam, The Netherlands

Tomohiro Suzuki
Flanders Hydraulics Research, Berchemlei 115, 2140 Antwerp, Belgium

Lorenzo Cappietti
Dip. di Ingegneria Civile e Ambientale, Università degli Studi di Firenze, Via S. Marta 3, 50139 Florence, Italy

ABSTRACT

Overtopping bore impact forces on a dike mounted vertical wall were measured in similar large-scale (Froude length scale factor 1-to-4.3) and small-scale (Froude length scale factor 1-to-25) models. The differences due to scale effects were studied, by comparing the up-scaled force measurements from both models in prototype. It was noted that if a minimum layer thickness, velocity of the overtopping flow and water depth at the dike toe were maintained in the small-scale model, the resulting differences in impact force due to scale effects are within the range of differences due to non-repeatability and model effects.

Keywords: scale effects, model effects, non-repeatability, laboratory experiments, bore impact force.

INTRODUCTION AND OBJECTIVES

In coastal engineering practice physical modelling is a widely used tool to better understand and solve issues related to wave transformation and wave-structure interaction. Large and expensive coastal structures are often tested before they are built, to study the fundamental processes and response to wave attack. Due to time constraints, feasibility, and economic concerns often a small-scale model of these coastal structures is tested instead of a prototype-scale version [1] and [2]. A scaled-down model of the prototype can be considered similar if the appropriate scaling laws are applied [2]. Maintaining similarity between the prototype and the model requires that the following conditions are met: 1) geometric similarity (similar in shape), 2) kinematic similarity (similar in motion) and 3) dynamic similarity (maintaining all force ratios). While the first two are often met, the third one requires a balance of inertial, gravitational, fluid friction, elastic compression, pressure and surface tension forces. A balance of all force ratios cannot be achieved; and therefore, scaling bias or scale effects will always exist when physical scale model tests are conducted [1] and [2]. Hence, it is important to consider the dominant forces to determine the correct scaling law. Typically, in situations where the dominant restoring force is gravity, Froude similarity or Froude scaling is applied [3]. In

[1] Maximilian.Streicher@UGent.be
[2] Previously affiliated with Ghent University

Froude scaling the balance between inertia and gravitational force is achieved, while all other force balances are assumed to be negligible. The Froude scaling factors, in terms of the length scale λ, for the investigated parameters of this study are given in Table 1.

Table 1. Froude scaling factors

Parameter	Froude scaling factor
Length [m]	λ
Time [s]	$\sqrt{\lambda}$
Force [kN/m]	λ^2

Froude scaling can become a source for unwanted scaling effects if air-water flow is modelled, such as with entrained and entrapped air in turbulent flows, because the difference in compressibility of the water between the model and prototype is not reliably accounted for with Froude scaling [3] and [4]. The authors also observed that the air-water void ratio was larger in prototype compared to the small-scale model and in salt water compared to fresh water. This means that any impact forces measured in small-scale are less damped due to lower compressibility of the fluid and so called cushioning of the impacts. Reference [5] showed the difference in air compressibility between different scale models numerically.

Previously, laboratory experiments were conducted for a scaled geometry similar to the Belgian coast, with a mildly sloping foreshore, shallow waters at the dike toe, a dike and attached to the dike a promenade, with a wall at the end [6], [7] and [8]. In the scale-models the overtopping wave impact forces against the wall were measured. When up-scaling the measured small-scale results without accounting for the changing compressibility of the fluid, the impact force in prototype is expected to be overestimated when Froude scaling is used. Additionally surface tension or viscous effects may play a role if the turbulent overtopping flow in the model becomes too small, which again is not accounted for with Froude scaling [9]. In this case these effects would result in additional friction and potentially a decrease of the flow in the small-scale model leading to a reduction of impact force: another source of scale effect.

In additional to scale-effects in small-scale laboratory experiments, model effects might also play a role and influence the obtained force measurement. Model and scale effects are often intertwined, such as with salt water in prototype and fresh water in the model, which is firstly a model effect but secondly also effecting the compressibility of the water and therefore the dynamic similarity and force balance related to scale effects. Other model effects are related to the wave generation and absorption mechanism or measurement techniques in the model [10]. The poor representation of the real sea-states and especially the long waves by using theoretical wave spectra in the model is another source of model effects [11]. Typically infra-gravity waves with prototype periods ~100-200s are difficult to reproduce in the small-scale models. The measurement system and choice of load cells itself influence the measurement as they are often less stiff in the small-scale model. Also the use of materials for the bathymetry, topography and load measurement plate (e.g. wood or metal) in the model influences the resulting force measurement if it does not behave (less or more smooth, erosion, stiffness etc.) similar to the prototype situation.

Another source for differences in impact force measurement is the stochastic behavior of the wave impact process itself and the resulting non-repeatability of overtopping wave impacts measurements [12] and [7]. Typically, this is explained by 3D effects of the turbulent bore front or small differences in air entrapment and entrainment in the impacting flow, which lead to unpredictable variations in the impact process and thus measured impact forces. An overview of factors causing differences in wave impact measurements in laboratory scale models is given in Table 2.

Table 2. Factors causing differences in wave impact force measurements in laboratory scale models

Non-Repeatability	Model effects	Scale effects
3D effects of turbulent bore front	Wave generation	Compressibility
Air entrainment	Wave absorption	Surface tension
Air entrapment	Load cell choice	Viscosity
	Measurement set-up	Water properties
	Water properties	Scaling law
	Material properties	

In this study the non-repeatability, model- and scale effects were further investigated. More detailed objectives are:

- to provide a detailed comparison of small-scale and large-scale model set-up and hydraulic boundary conditions, in order to discuss similarity of the two models.
- to investigate potential model effects in terms of absolute and percentage difference between spectral wave parameters at the dike toe, for the two models.
- to investigate the non-repeatability of wave impact force measurements using the small-scale model and same time-series of waves in order to establish a baseline uncertainty against which the scale effects can be judged.
- to investigate scale effects of impact force measurements by comparing the force measurements from the small-scale and large-scale model in prototype-scale values and to discuss the absolute and percentage difference of the force indicators F_{max}, $F_{1/250}$, $F_{10\%,}$, F_{10}, F_{20}, F_{30}, F_{50}, F_{100}, $F_{avg.}$

MODEL SET-UP AND HYDRAULIC BOUNDARIES

The model geometry was a scaled representation of a large part of the bathymetry and topography of coasts from low-lying countries and comprised of four elements (Figure 1): 1) a mildly sloping foreshore with shallow waters at the dike toe, 2) a dike connected to, 3) a promenade, and at the end of the promenade, 4) a vertical wall.

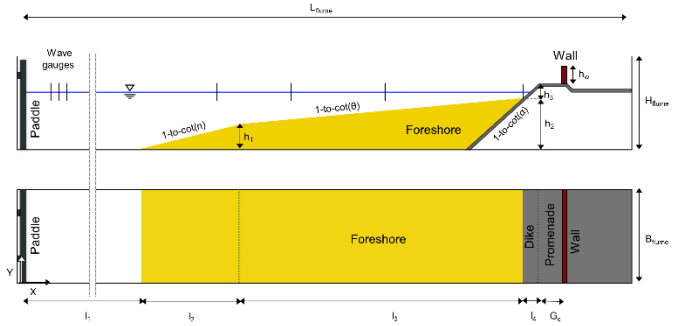

Figure 1. Side-view (upper figure) and top-view (lower figure) sketch of the model geometry

For this study two scale models of this geometry were tested in two different test series. The Large-scale (Froude length scale factor 1-to-4.3) experimental campaign was conducted within the research project WALOWA, carried out in the Delta Flume in March 2017 [12]. It is herein referred to as the large-scale experiment. The small-scale (Froude length scale factor 1-to-25) experimental campaign was conducted in Spring 2018. It is herein referred to as the small-scale experiment. The scale ratio between the two scale models was 1-to-5.81.

1.1 Large- and small-scale model set-up

Hereafter, only a compact overview of the geometry has been summarized with a focus on the main differences (Table 3). For better comparability all dimensions were up-scaled to prototype scale using Froude similarity.

Most striking differences between the two scale models can be found in the distance between the wave paddle and the start of the foreshore. While the prototype-scale distance was 404.1m for the large-scale model, it was only 274m in the small-scale model. As a result of the length difference the wave propagation and interaction with reflected waves was altered, leading to a different water surface elevation time series at the toe of the dike.

Furthermore, the applied foreshore material in the large-scale model was sand with a grain size diameter of D_{50} = 320µm. In the small-scale model smooth concrete was used to build the foreshore. It was expected that on the one hand the porosity of the sand will lead to additional wave energy dissipation and on the other hand the erosion of sand at the dike toe will lead to larger water depths h_t and potentially higher wave energy at the toe of the dike [14]. Regardless of the scour hole at the dike toe, which developed for the sand foreshore, the dike toe location and water depth at the dike toe h_t were defined at the connecting point between initial foreshore geometry and dike.

Table 3. Comparison of wave flume and model dimensions between large-scale and small-scale experiment. Values were up-scaled and compared in prototype scale

	Small-scale (SS)	Large-scale (LS)
Model scale	1-to-25	1-to-4.3
Flume	Ghent University	Delta Flume
	L = 750m H = 30m W = 25m	L = 1251.3m H = 40.85m W = 21.5m
Foreshore	concrete	sand
	cot(n) = 10 cot(θ) = 35 l_1 = 274m l_2 = 83.9m l_3 = 264.9m	cot(n) = 10 cot(θ) = 35 l_1 = 404.1m l_2 = 83.9m l_3 = 264.9m
Dike	plywood	concrete
	cot(α) = 2 h_3 = 2.3m	cot(α) = 2 h_3 = 2.3m
Promenade	plywood	concrete
	G_c = 10m	G_c = 10m
Wall	alluminium plate	hollow steel profile
	h_w = 6.88m not overtopped	h_w = 6.88m not overtopped
Force	Tedea-Huntl. 5kN fs = 1000Hz	HBM U9 20 kN fs = 1000Hz

Dike and promenade were constructed from plywood in the small-scale model and concrete in the large-scale model. It was expected that the slightly smoother plywood would result in

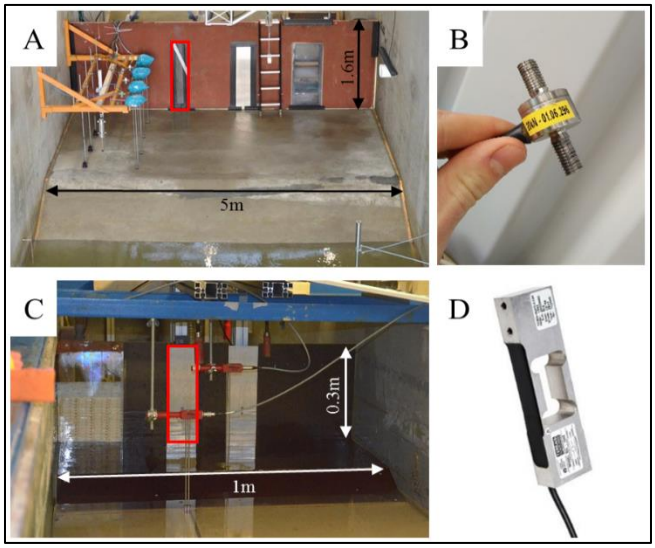

Figure 2. Dike, promenade and wall in large-scale (A) and in small-scale (C). The impact forces were measured in the area highlighted in red, with two compression load cells in large-scale (B) and a strain gauge load cell in small-scale (D).

lower friction losses of the overtopping water flow in the small-scale model. In both scale models the wall was high enough to prevent overtopping by the run-up water.

The impact forces were measured with two HBM U9 compression load cells with a measurement range of 20kN in the large-scale model (Figure 2, A and B). The maximum absolute error was 0.007 kN and the maximum relative error 0.363% of the full-scale output. The load cells were connected above each other to the same 0.2m-wide hollow steel profile. The profile was flush-mounted into the wall (red rectangle). The resonance frequency of the large-scale measurement system was estimated to be approximately at 80Hz. In the small-scale model the impact forces were measured using a Tedea-Huntleigh strain gauge load cell with a measurement range of 5kN (Figure 2, C and D). The maximum relative error was stated as 0.02% of the full-scale output. The strain gauge load cell was connected to a 0.1m-wide aluminum plate, and the plate flush-mounted with the rest of the wall (red rectangle). A static calibration of this instrument was roughly done by placing defined weights on the load cell and measuring the weight response. The first resonance frequencies of the small-scale measurement system were found at 35Hz, 45Hz and 53Hz.

All other parameters, such as the crest freeboard, A_c, and the offshore water depth, h_o, were kept the same. The comparison of the wave time-series and spectral parameters at a location close to the paddle and at the dike toe location provided further insight into whether similarity of the hydraulic boundary conditions between the two scale models was achieved.

1.2 Large- and small-scale wave parameters

Waves were generated in both scale models with a piston-type wave paddle. Two tests with wave conditions similar to a storm with a 1-in-1000 (Irr_4_F) and 1-in-17000 (Irr_1_F) return interval [15] were selected for this study.

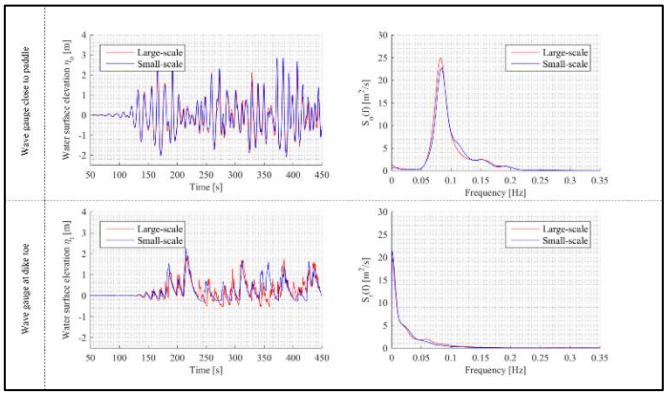

Figure 3. Beginning of the water surface elevation time-series (left) and wave spectrum calculated for the entire time-series (right) for test Irr_1_F in the small-scale (blue) and large-scale (red) model and for the offshore (upper row) and dike toe (lower row) location. Values are in prototype-scale units.

The steering signal in the small-scale model was the down-scaled measured time-series of waves from the large-scale model. In this way a most similar sequence of waves in both scale models was achieved. The active wave absorption system was activated in both scale model experiments.

The water surface elevation η(t) was measured with resistive type wave gauges deployed at the flume wall for the large-scale model and in the middle of the flume for the small-scale model. The measurement location in flume length direction was the same between scale models, and this location was referred to as the offshore location (above the flat bottom part in the flume and before the start of the foreshore) and as the dike toe location. Spectral wave parameters at the offshore location H_{m0_o} [m] and $T_{m-1,0\_o}$ [s] and at the dike toe location H_{m0_t} [m] and $T_{m-1,0\_t}$ [s] were obtained for test Irr_1_F (Table 4) and test Irr_4_F (Table 5) in both scale models. The spectral analysis was performed using similar analysis settings. Low cut-off and high cut-off frequencies were the scaled equivalent of each other using the scale ratio 1-to-5.81. A low cut-off frequency at 3Hz (large-scale model) and 7Hz (small-scale model), as well as a high cut-off frequency at 0.025Hz (large-scale model) and 0.060Hz (small-scale model).

The ratio for the offshore spectral wave height and period between large-scale and small-scale experiment was in the order of ~1% and ~3% respectively for test Irr_1_F (Table 4). This was considered acceptable and confirmed by the good agreement between the large-scale and small-scale time-series of water surface elevation η (Figure 3, upper row). However, the ratio of spectral wave height and period at the dike toe between large-scale and small-scale experiment was in the range of ~10% for test Irr_1_F. This was confirmed by the slightly worse agreement between large-scale and small-scale time-series of water surface elevation η at the dike toe (Figure 3, lower row).

Table 4. Hydraulic boundary conditions test Irr_1_F. The values were up-scaled and compared in prototype.

IRR_1_F	Small-scale (SS)	Large-scale (LS)	Ratio (SS/LS)
Model scale	1-to-25	1-to-4.3	1-to-5.81
$H_{m0,o}$ [m]	4.64	4.59	1.011
$T_{m-1,0,o}$ [s]	11.67	12.03	0.970
$H_{m0,t}$ [m]	2.79	2.51	1.112
$T_{m-1,0,t}$ [s]	37.03	33.42	1.108
Duration [s]	~13000	~13000	-
h_o [m]	17.25	17.16	1.005
h_t [m]	1.3	1.21	1.074
A_c [m]	1	1.08	0.926

There were more shorter waves visible in the large-scale model time-series at the dike toe location.

The same analysis was performed for test Irr_4_F. The ratio for the offshore spectral wave height and period between large-scale and small-scale model was on the order of ~2% and was considered to be in good agreement (Table 5). The ratio of spectral wave height and period at the dike toe between large-scale and small-scale model was again in the order of 7% and 10% respectively. It is striking that the wave height at the dike toe in the small-scale model was lower than in the large-scale model. This difference could possibly be explained by the

increased water depth at the dike toe due to the fully developed erosion hole in the large-scale model (~0.15m in model scale and 0.65m in prototype [15]), because the test was conducted at a later time during the experimental campaign, while Irr_1_F was conducted in the beginning of the experimental campaign, with less erosion at the dike toe [13].

Table 5. Hydraulic boundary conditions test Irr_4_F. The values were up-scaled and compared in prototype.

IRR_4_F	Small-scale (SS)	Large-scale (LS)	Ratio (SS/LS)
Model scale	1-to-25	1-to-4.3	1-to-5.81
$H_{m0,o}$ [m]	3.76	3.81	0.987
$T_{m-1,0,o}$ [s]	10.89	11.11	0.980
$H_{m0,t}$ [m]	1.74	1.87	0.930
$T_{m-1,0,t}$ [s]	32.54	29.70	1.096
Duration [s]	~12000	~12000	-
h_o [m]	16.25	16.30	0.997
h_t [m]	0.30	0.34	0.882
A_c [m]	2	1.94	1.031

The agreement of the water surface elevation time-series and spectral distribution between small-scale and large-scale model was considered good at the offshore location (Figure 4, upper row). Comparable to test Irr_1_F the agreement is worse at the dike toe location (Figure 4, lower row). Additionally it was noted that the number of small waves was higher for the large-scale model tests and the dike toe location in both tests.

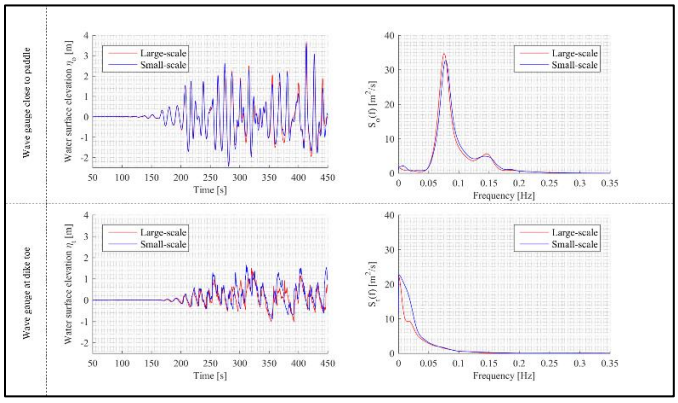

Figure 4. Beginning of the water surface elevation time-series (left) and wave spectrum calculated for the entire time-series (right) for test Irr_4_F in the small-scale (blue) and large-scale (red) model and for the offshore (upper row) and dike toe (lower row) location. Values are in prototype.

Whereas a difference of ~1-3% in spectral wave parameters at the offshore location seems negligible, the difference of ~10% for the dike toe location becomes more significant for both tests and should be considered when interpreting the results of the impact measurements. Furthermore, the larger number of waves at the dike toe location in the large-scale model will increase the number of impacts at the wall as well.

DATA ANALYSIS AND RESULTS

Just as for the geometrical model set-up and hydraulic boundary conditions, care was taken to make the data processing of the large-scale and small-scale impact force measurements as similar as possible. In this way additional model effects due to different data processing routines were minimized, and the investigation of scale effects enabled.

1.1 Filtering of impact force measurements

The time-series of measured impact force at the wall was recorded at 1000Hz in both scale models. It was further attempted to down-sample the measurement frequency of the large-scale model, using Froude similarity and the scale ratio 1-to-5.81, to artificially create a similar measurement frequency used in the small-scale model. In this way the 1000Hz signal of the large-scale model was interpolated and a 415Hz signal obtained. No significant reduction of the force peaks was observed, and it was decided to use the original 1000Hz measurement signals.

The obtained time series for test Irr_1_F and test Irr_4_F in both scales was post-processed in three steps using Matlab® software. First, removing drift and applying zero-offset corrections to the measured signal were attempted. Also, filtering, to remove phenomena related to model effects (electronic current frequency or resonance frequency of the measurement system), was carried out in frequency domain. A low-pass butterworth filter 5th order at 48 Hz in large-scale model. This filter was downscaled to the small-scale model dimensions using Froude similarity and a scale factor of 1-to-5.81. This resulted in a similar low pass filter at 115Hz for the small-scale model. The low-pass filter was chosen as a compromise between preserving the short duration impulsive impacts and limiting the decrease in peak impact force (typically around 10-20% [17]). Also band-stop filters to remove the induced resonance frequencies of the measurement systems (80Hz in large-scale model and 35Hz, 45Hz, 53Hz in small-scale model) were applied. Additionally a band-stop filter to filter out the noise from the electronic current system (at 50Hz) was used. Secondly, the signals of the two load cells attached to the same measurement hollow steel profile in large-scale were added. The sum was divided by the width of the measurement plate to obtain a force per meter width value. In the small-scale model the load cell signals were simply divided by the width of the measurement plate to obtain a force per meter width value. Third, a half-automatic peak detection method was applied and the key events from the filtered time-series selected. A minimum time between force peaks was set to 2s in large-scale and 0.83s (downscaled) in small-scale. accordingly. Additionally, a high-pass threshold in time domain for the force peaks was set as low as the noise level of the measurement would allow. Previously, [17] used the mean wave power as proposed by [18] to define a high-pass threshold for the force peaks. The mean wave power is defined as $\frac{1}{8} * \rho * g * {H_{m0,toe}}^2$ and was used in the present study to define the high-pass threshold for the force peaks in time domain.

1.2 Non-repeatability of impact force measurements

It is commonly accepted that wave impact measurements are highly stochastic and non-repeatable [7] and [12]. The non-repeatability was mainly attributed to 3D effects of the turbulent bore front, air entrapment during wave impact, and air entrainment in the turbulent bore front. Hence, it was attempted to quantify the non-repeatability of wave impacts in order to establish a baseline uncertainty against which the model and scale related differences in measured impact force can be compared. For this purpose the irregular wave time-series of test Irr_4_F (Table 5) was repeatedly (14 times) tested in the small-scale model. The results for the impact force were up-scaled to prototype scale and the time-series as well as the statistical parameters studied (Figure 5).

The same time-series of waves was used in each repetition test, resulting in a relative mean difference of the spectral wave height $H_{m0,t}$ and period $T_{m-1,0,t}$ at the dike toe of less than 0.5%. Even though the same time-series of waves showed good repeatability, the impact forces varied greatly. The maximum impact force per test was measured at different times in between repetition tests and varied significantly in magnitude (Figure 5, upper figure). A zoom into the impact event which caused the maximum impact force in most tests (t = ~2000s) was provided and showed the general shape of this impact event for the 14 repetition tests (Figure 5, lower left figure).

Furthermore, the mean value μ, the standard deviation σ and coefficient of variation $C_v = \sigma/\mu$ were computed for the 14 repetition tests, to quantify the uncertainty. These statistical parameters were derived for the force indicators: maximum impact force F_{max}, average 1-in-250 impact force $F_{1/250}$, average of the highest 10% of impact forces $F_{10\%,}$, average of the highest 10, 20, 30 impact forces F_{10}, F_{20}, F_{30}, respectively and average of all impact forces F_{avg} (Table 6).

Table 6. Statistical parameters showing the differences in measured impact force due to the stochastic impact behavior

	μ [kN/m]	σ [kN/m]	C_v [%]	$\bar{D}$ [%]
F_{max}	14.10	1.44	10.21	8.41
$F_{1/250}$	14.10	1.44	10.21	8.41
$F_{10\%}$	9.36	0.57	6.09	4.57
F_{10}	8.57	0.48	5.60	4.10
F_{20}	6.20	0.32	5.16	4.36
F_{30}	4.97	0.26	5.23	4.27
F_{avg}	2.48	0.13	5.24	4.58

The coefficient of variation C_v was around 10% for the maximum impact force F_{max} (and the same for $F_{1/250}$, because there were only 46 total impact events). The coefficient of variation was in the order of ~5.5% for the other force indicators ($F_{10\%,}$ F_{10}, F_{20}, F_{30}, F_{avg}). Additionally, the average deviation from the mean was computed as $\bar{D} = \sum_{i=1}^{14}[\mu - F_i]/\mu \cdot 100$. The values were in the range of the coefficient of variation C_v with ~8% for F_{max} and $F_{1/250}$ and ~4.5% for the other force indicators (Table 6). The deviation of the mean for each of the 14 repetition tests was calculated and a boxplot generated (Figure 5, lower right figure).

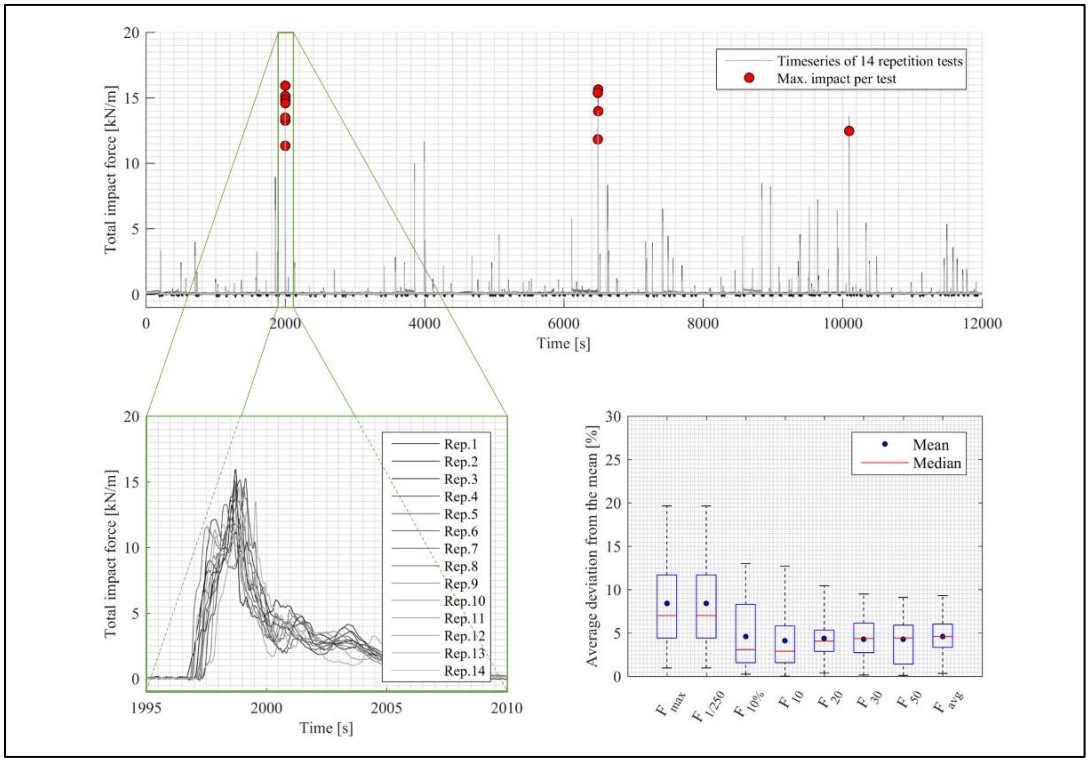

Figure 5. Force time-series of 14 repetition tests (upper figure) with the maximum impact force per time-series (red marker). Zoom on the impact event around t=2000s (lower left figure) and boxplot of deviations from the mean impact force (lower right figure).

The boxplot provides the additional information that even though the average deviation from the mean is around 8% there are single repetition tests with a deviation from the mean in the order of 20% for F_{max} and $F_{1/250}$, as can be seen from the upper outliers in the boxplot. It was therefore concluded that the relative uncertainty related to the non-repeatability of the maximum impact force for an irregular wave train was 10% for the maximum impact force and could go up to 20% in extreme cases. This is in the range of coefficient of variations C_v for quasi-static and dynamic impact forces measured with load cells, in a regular wave train and estimated as 10% and 14%, respectively by [7].

1.3 Scale-effects of impact force measurements

To study the small-scale and large-scale impact force measurement for test Irr_1_F (Table 4) the time-series of impact force were up-scaled and compared in prototype scale. Froude length scale factors of 1-to-4.3 (large-scale) and 1-to-25 (small-scale) were used. First, the time-series were synchronized by shifting one time series relative to the other to obtain the visual best-fit overlay. This allowed qualitative study of the number of occurrences and magnitude of impact events (Figure 6, upper figure). It was noted that there were less impact events recorded in small-scale (424 impact events) than in large-scale (549 impact events). Also, in terms of magnitude it was observed that the same event in time differed significantly in between both scale models. Furthermore the maximum impact was not recorded at the same time in the two scale models. The distribution of the impact events showed that the small-scale model results were higher in magnitude compared to the large-scale model results (Figure 6, lower left figure). On the x-axis the total impact force for each impact event was plotted in force per meter width, and the y-axis shows the corresponding exceedance probability. As described earlier the mean wave power after [18] was used to define the high-pass threshold. The same force indicators as in the non-repeatability study were used (Figure 6, lower right figure). In all cases the small-scale model force indicator was higher than the according large-scale model force indicator (Table 7).

Table 7. Force indicators from large-scale and small-scale measurements compared in prototype for test Irr_1_F

IRR_1_F	Small-scale (SS)	Large-scale (LS)	Ratio (SS/LS)
Nr. of impacts [-]	424	549	0.772
F_{max} [kN/m]	86.97	83.87	1.037
$F_{1/250}$ [kN/m]	84.96	77.88	1.091
$F_{10\%}$ [kN/m]	51.86	40.33	1.286
F_{10} [kN/m]	70.97	65.70	1.080
F_{20} [kN/m]	62.98	55.55	1.134
F_{30} [kN/m]	57.30	49.56	1.156
F_{50} [kN/m]	49.69	42.22	1.177
F_{100} [kN/m]	39.08	32.01	1.221
F_{avg} [kN/m]	15.78	11.79	1.338

The relative difference between small-scale and large-scale model force indicator was calculated. The maximum impact

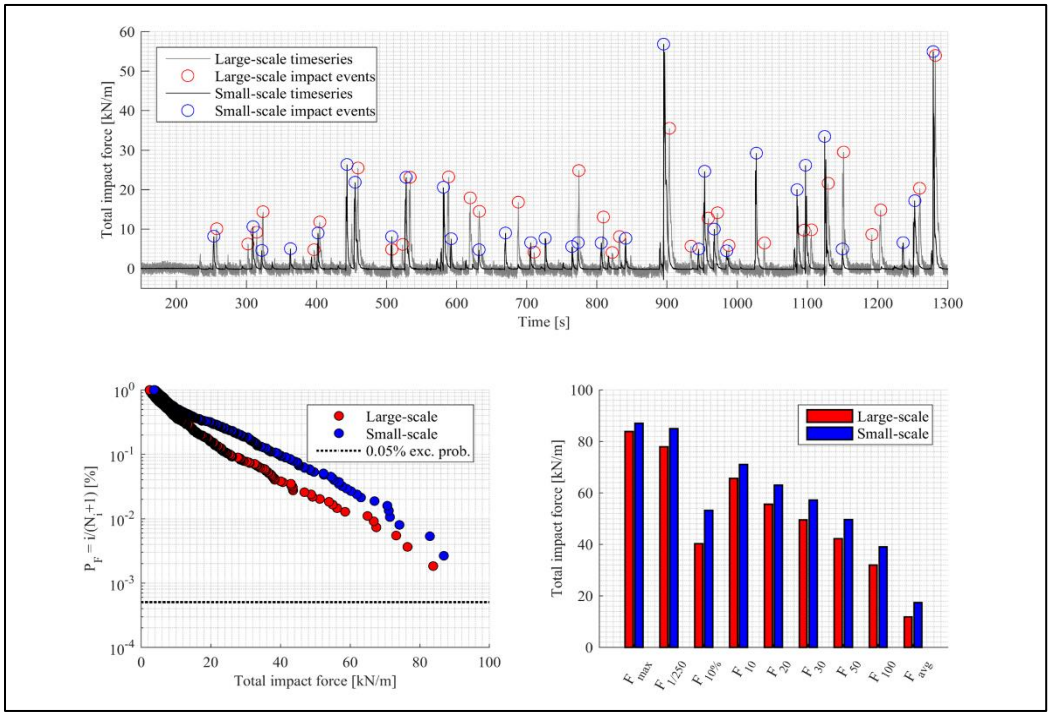

Figure 6. Beginning of time-series of impact forces for test Irr_1_F (upper figure), in red the large-scale and in blue the small-scale impact events. Impact force event distribution (lower left figure) and comparison of force indicators (lower right figure).

force F_{max} was ~4% higher in the small-scale model, the average impact force $F_{1/250}$ was ~9% higher in the small-scale model (Table 7). The other force indicators were ~8-34% higher in the small-scale model.

The same analysis was repeated for test Irr_4_F (Table 5). For the time-series of impact force (Figure 7, upper figure) it was noted that the relative difference in the number of impact events between small-scale (46 impact events) and large-scale (103 impact events) was higher compared to test Irr_1_F. The distribution of the impact events showed that the small-scale model results were only higher for exceedance probabilities between $5 \cdot 10^{-2}$ – $3 \cdot 10^{-1}$ and that the large-scale model results showed the highest impact force. The maximum impact forces were lower compared to test Irr_1_F due to the less severe wave conditions. A study of the force indicators showed that all of them, contrary to the findings for test Irr_1_F, were higher in the large-scale model (Figure 7, lower right figure). The relative difference for F_{max} and $F_{1/250}$ was 19%, with higher values in the large-scale model (Table 8). Note that the result for F_{max} and $F_{1/250}$ were the same because only 46 or 103 impact events were recorded. Furthermore, the large-scale results were 3-30% higher for the other force indicators. The F_{50} and F_{100} force indicators could not be compared due to the insufficient number of impact events.

Whereas the results for test Irr_1_F were in line with the widely accepted narrative of an overestimation of wave impacts in small-scale models, the results for test Irr_4_F were contradictory.

Table 8. Force indicators from large-scale and small-scale measurements compared in prototype for test Irr_1_F

IRR_4_F	Small-scale (SS)	Large-scale (LS)	Ratio (SS/LS)
Nr. of impacts [-]	46	103	0.447
F_{max} [kN/m]	16.66	20.57	0.810
$F_{1/250}$ [kN/m]	16.66	20.57	0.810
$F_{10\%}$ [kN/m]	10.67	11.78	0.906
F_{10} [kN/m]	9.61	12.15	0.791
F_{20} [kN/m]	6.99	9.30	0.752
F_{30} [kN/m]	5.53	7.83	0.706
F_{avg} [kN/m]	4.19	4.31	0.972

On the one hand it was assumed that this was the result of the larger spectral wave height $H_{m0,t}$ at the dike toe (10% higher in large-scale) due to the formation of the erosion hole (0.15m in model scale and 0.65 in prototype scale [15]); and consequently, larger water depth at the dike toe. Higher energy waves could transform up to the dike toe leading to more overtopping and finally more, and potentially higher, impact events at the wall. Furthermore, the water depths at the dike toe in test Irr_4_F were $h_t < 0.02$m in the small-scale, which means that effects of surface tension may not have been negligible during wave transformation [9]. On the other hand the overtopping flow thicknesses and velocities on the promenade were rather small for test Irr_4_F. Consequently, effects due to viscosity and

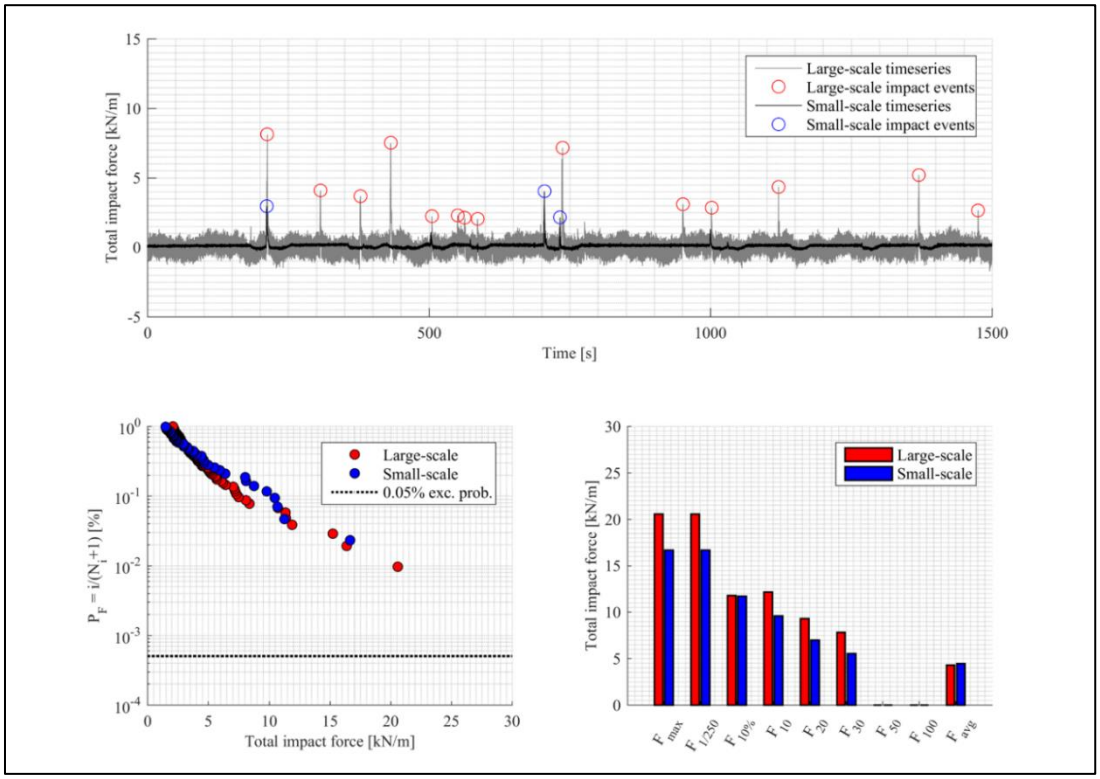

Figure 7. Beginning of time-series of impact forces for test Irr_1_F (upper figure), in red the large-scale and in blue the small-scale impact events. Impact force event distribution (lower left figure) and comparison of force indicators (lower right figure).

surface tension, neglected in the Froude up-scaling, might influence the results. It was previously stated that for flow depths $\eta_{crit} < 0.0035$m [19], Reynolds number $Re_{crit} < 1000$ and Weber number $We_{crit} < 10$ [9] the flow becomes hydraulic smooth and the resistance due to viscosity and surface tension will further decrease or stop the flow. Measurements of the flow thickness η [m] and velocity u [m/s] on the promenade were obtained for the 30 highest impacts of test Irr_4_F in the large-scale model [20] and [21]. No flow thickness and velocity was measured in the small-scale model. As a first estimate for the flow thickness η [m] and velocity u [m/s] in the small-scale model the large-scale results were down-scaled using Froude length scale and the scale ratio 1-to-5.81. While the Reynolds numbers Re in the so obtained small-scale results were in the range Re = 4221-27724 and above the critical $Re_{crit.}$=1000, the Weber numbers were in the range of We = 22-310 and closer to the critical We_{crit} = 10. However, this comparison is very tentative, and the analysis of measured flow thickness η [m] and velocity u [m/s] in the small-scale model need to be studied. Due to the combination of model effects (erosion hole at dike toe in large-scale) leading to higher wave energy at the dike toe and unresolved scale effects due to the size of the flow thicknesses and velocities in the small-scale model test Irr_4_F, no further study of wave impact force scale effects was conducted based on test Irr_4_F .

For test Irr_1_F the small-scale model showed a small systematic shift towards higher force impacts compared to the large-scale model. Also the force indicators F_{max}, $F_{1/250,}$ etc, were systematically higher (3%-34%). Anyhow, the overestimation of forces in the small-scale model was judged to be not remarkably high, especially for F_{max} and $F_{1/250}$. The Reynolds and Weber number of the overtopping flow related to the 30 highest events were well above the critical Reynolds and Weber number. Hence, scale effects related to viscosity and surface tension of the overtopping flow were considered negligible. Typically, the overestimation of impact force in smaller scale models was explained by the lower amount of entrained air and the resulting lower cushioning effect during the impact process. In the case of overtopping wave impacts, the waves reaching and impacting the dike-mounted wall were all broken; and no violent plunging wave breaking was observed, in contrast to plunging wave breaking on seawalls constructed in the breaking zone. Hence, the cushioning effect was less effective because the wave impacts were less violent and of rather quasi-static nature [20]. Therefore, the error induced due to Froude scaling was expected to be rather small [22]. Nevertheless, , no such air entrainment was measured during the experiments, and it remains an assumption that the small systematic shift to higher forces in the small-scale model was a result of the lower amount of entrained air.

The difference in impact force between the scale models could also be explained by the difference in spectral wave parameters at the dike toe, which were ~10% higher in the small-scale model. The long waves were less efficiently absorbed in the small-scale model, and this resulted in this increase in spectral wave parameters at the dike toe. The underlying assumption here would be that 10% higher spectral wave parameters will result in a systematical shift of 3%-34% higher impact forces.

In any case, the observed higher impact forces in the small-scale model, especially for F_{max}, $F_{1/250}$, F_{10}, F_{20}, F_{30} were in the range of 3%, 9%, 8%, 13%, 16%, respectively. Compared to the uncertainties from the non-repeatability study, which showed an average deviation of ~10% and in extreme cases of ~20% for the maximum impact force F_{max}, the scale-effect related error, possibly due to air entrainment, was considered subordinated. Adding also the average reduction of force peaks 10-20% [17] due to filtering of the impact forces, the scale related error disappears within the uncertainties caused by the non-repeatability and model effects.

CONCLUDING REMARKS

In this study the non-repeatability, model- and scale effect for laboratory impact load measurements induced by an overtopping bore on a dike mounted wall were investigated. The main conclusions of this study were:

- If a minimum water depth at the dike toe, as well as thickness and velocity of the overtopping flow are maintained, the scale-related errors in the impact force measurement disappear within the uncertainties related to non-repeatability and model effects.
- The above finding was contradictory to the assumption that force measurements in the small-scale model are significantly higher than prototype measurements. The contradiction was mainly explained by the characteristics of the turbulent, aerated and broken bore impacts, resulting in compressible and less violent impacts. Note this impact behavior was very different compared to violent breaking wave impacts on seawalls constructed in the breaking zone. Also, the relative scale ratio between the two models was rather low with 1-to-5.8.
- However, a small systematic scale-related shift to higher impact forces was observed in the order of 4%, 9%, 8%, 13%, 16% for F_{max}, $F_{1/250}$, F_{10}, F_{20}, F_{30} respectively, in the small-scale model. Furthermore, the number of impacts was lower in the small-scale model (424) compared to the large-scale model (549).
- The uncertainties related to the non-repeatability of impact forces were quantified using the coefficient of variation and were in the order of 10% (in extreme cases up to 20%) for F_{max} and $F_{1/250}$.
- Differences related to model effects were mostly observed in the wave generation and absorption in the small-scale model and changing sand bathymetry in the large-scale model. On average this resulted in 10% difference in spectral wave parameters at the dike toe location between the two scale models.

For future studies on scale effects related to overtopping bore impacts on dike mounted walls, it is recommended to further advance the wave generation and wave absorption in the small-scale model to better represent the long wave characteristics. Additionally, measurements of air entrainment in

both scales, at a location close to the wall where the impact force occurs, would be beneficial to judge the difference in flow aeration between different scale models. The use of pressure sensors in both scale models is recommended to further study the scale influence on peak impact pressures. Furthermore, extra intermediate scale models or fully prototype-scale measurements could be used to judge whether the bore impacts scale linearly and to increase the relative scale difference.

ACKNOWLEDGEMENTS

The work described in this publication was supported by the European Community's Horizon 2020 Research and Innovation Programme through the grant to HYDRALAB-PLUS, Contract no. 654110.

REFERENCES

[1] Heller, V., 2011. "Scale effects in physical hydraulic engineering models", Journal of Hydraulic Research, Vol. 49, 293-306.

[2] Frostick, L., McLelland, S., Mercer, T., 2011. "User Guide to Physical Modelling and Experimentation: Experience of the HYDRALAB Network", Leiden, The Netherlands: CRC Press/Balkema.

[3] Bullock, G.N., Hewson, P.J., Walkden, M.J.A., Bird, P.A.D., 2001. "The influence of air and scale on wave impact pressures", Coastal Engineering, Vol. 42, 291-312.

[4] Blenkinsopp, C., Chaplin, J., 2011. „Void fraction measurements and scale effects in breaking waves in freshwater and seawater", Coastal Engineering, Vol. 58, 417-428.

[5] Simonetti, I., Cappietti, L., Elsafti, H., Oumeraci, H., 2018. „Evaluation of air compressibility effects on the performance of fixed OWC wave energy converters using CFD modelling", Renewable Energy, Vol. 119, 741-753. doi 10.1016/j.renene.2017.12.027.

[6] Van Doorslaer, K., A. Romano, J. De Rouck, A. Kortenhaus. 2017. "Impacts on a storm wall caused by non-breaking waves overtopping a smooth dike slope", Coastal Engineering, Vol. 120, 93-111, doi: 10.1016/j.coastaleng.2016.11.010.

[7] Chen, X. 2016. "Impacts of overtopping waves on buildings on coastal dikes", PhD diss., TU Delft, doi: 10.4233/uuid:e899b6e4-fcbe-4e05-b01f-116901eabfef.

[8] Streicher, M., Kortenhaus, A., Hohls, C., 2016. "Analysis of post overtopping impacts on a vertical wall at the Belgian coast", 6th Coastlab conference, Ottawa, 1-10.

[9] Schüttrumpf, H. 2001. Wellenüberlaufströmung an Seedeichen – Experimentelle und theoretische Untersuchungen, PhD diss., TU Braunschweig.

[10] Hughes, S.A., 1995. "Physical Models and Laboratory Techniques in Coastal Engineering", Advanced Series on Ocean Engineering. Vol. 7. World Scientific.

[11] Oumeraci, H., Schüttrumpf, H.; Sauer, W., Möller, J., Droste, T., 2000. „Physical Model Tests on Wave Overtopping with Natural Sea States", LWI-Bericht Nr. 852.

[12] Verwaest, T., Altomare, C., Suzuki, T., Trouw, K., 2014. "Characterization of wave impacts on curve faced storm return walls within a stilling wave basin concept", 34th International conference on coastal engineering, 1-12, https://doi.org/10.9753/icce.v34.structures.57.

[13] Streicher, M., A. Kortenhaus, C. Altomare, V. Gruwez, B. Hofland, X. Chen, K. Marinov, B. Scheres, H. Schüttrumpf, M. Hirt, L. Cappietti, A. Esposito, A. Saponieri, N. Valentini, G. Tripepi, D. Pasquali, M. D. Risio, F. Aristodemo, L. Damiani, M. Willems., D. Vanneste, T.Suzuki, M. Klein Breteler, D. Kaste. 2017. „WALOWA (Wave Loads on Walls) – Large-scale experiments in the Delta Flume", Proceedings of the 8th SCACR conference, Santander, Spain, 1-11, doi: 10.5281/zenodo.834874.

[14] Hofland, B., Chen, X., Altomare, C., Oosterlo, P., 2017. „Prediction formula for the spectral period $T_{m-1,0}$ on mildly sloping shallow foreshores" *Coastal Engineering* Vol. 123, 21-28, doi: 10.1016/j.coastaleng.2017.02.005.

[15] Saponieri, **A.,** Di Risio, M., Pasquali, D., Valentini, N., Aristodemo, F., Tripepi, G., Celli, D., Streicher, M., Damiani, L., 2018. "Beach profile evolution in front of storm seawalls: A physical and numerical study", 36th International conference on coastal engineering, Baltimore, US, 1-13

[16] Veale, W., Suzuki, T., Verwaest, T., Trouw, K., Mertens, T., 2012. "Integrated design of coastal protection works for Wenduine Belgium", Proceedings of the 33rd International conference on coastal engineering, Santander.

[17] Chen, X., Hofland, B., Uijttewaal, W., 2016. "Maximum overtopping forces on dike-mounted wall with a shallow foreshore", Coastal Engineering, Vol. 116, 89-102.

[18] Goda, Y., 2010. "Random seas and design of maritime structures".

[19] Kolkman, P.A., 1984. „Consideration about the Accuracy of Discharge Relations of Hydraulic Structures and the Use of Scale Models for their Calibration", Symposium on Scale Effects in Modelling Hydraulic Structures. Esslingen. S. 2.1-1 - 2.1-12.

[20] Streicher, M., Kortenhaus, A., Marinov K., Hirt, M., Hughes, S., Hofland, B., Scheres, B., Schüttrumpf, H., 2019. „Classification of bore patterns induced by storm waves overtopping a dike crest and their impact types on dike mounted vertical walls – A large-scale model study", Coastal Engineering Journal, doi: 10.1080/21664250.2019.1589635.

[21] Cappietti, L., Simonetti, I., Esposito, A., Streicher, M., Kortenhaus, A., Scheres, B., Schuettrumpf, H., Hirt, M., Hofland, B., Chen, X., 2018. „Large-scale experiments of wave-overtopping loads on walls: Layer thicknesses and velocities", 37th International conference on ocean, offshore and arctic engineering, Madrid, Spain, p.6.

[22] Kortenhaus, A., Oumeraci, H. 1999. "Scale effects in modelling wave impact loading of coastal structures", Hydralab-workshop on experimental research and synergy effects with mathematical models, Leibniz-Haus, Hannover, Germany, p.10.

DISCLAIMER

